International Journal of Nanomedicine

Dovepress
open access to scientific and medical research

Open Access Full Text Article

ORIGINAL RESEARCH

Microporous elastomeric membranes fabricated with polyglycerol sebacate improved guided bone regeneration in a rabbit model

This article was published in the following Dove Medical Press journal:
International Journal of Nanomedicine

Bo Jian[1,2]
Wei Wu[2]
Yingliang Song[1]
Naiwen Tan[3]
Chao Ma[1]

[1]State Key Laboratory of Military Stomatology, Department of Implant Dentistry, School of Stomatology, The Fourth Military Medical University, Xi'an, Shaanxi, 710032, China; [2]Department of Oral & Maxillofacial Surgery, School of Stomatology, The Fourth Military Medical University, Xi'an, Shaanxi, China; [3]Department of Stomatology, Hospital 463 of PLA, Shenyang, Liaoning, People's Republic of China

Purpose: We aimed to fabricate guided bone regeneration (GBR) membrane using polyglycerol sebacate (PGS) and investigate the impact of scaffold pore size on osteogenesis.

Materials and methods: PGS microporous membrane was fabricated by salt-leaching technique with various pore sizes. Twenty-eight male New Zealand rabbits were randomly divided into four groups: 25 μm PGS membrane, 53 μm PGS membrane, collagen membrane, and blank control group. Subsequently, standardized and critical-sized tibia defects were made in rabbits and the defective regions were covered with the specifically prepared membranes. After 4 and 12 weeks of in vivo incubation, bone samples were harvested from tibia. Micro-computed tomography scanning was performed on all bone samples. A three-dimensional visible representation of the constructs was obtained and used to compare the ratios of the ossifying volume to total construct volume (bone volume to tissue volume [BV/TV]) of each sample in different groups; then, bone samples were stained with H&E and Masson's trichrome stain for general histology.

Results: At 4 weeks, the BV/TV in the 25 μm PGS group was found higher than that in the 53 μm PGS and collagen groups. At 12 weeks, the bone defect site guided by the 25 μm PGS membrane was almost completely covered by the new bone. However, the site guided by the 53 μm PGS membrane or collagen membrane was covered only most of the defects and the left part of the defect was unoccupied. Histological observation further verified these findings.

Conclusion: We thus concluded that the 25 μm PGS membrane played an advantageous role during 4–12 weeks as compared with those earlier degraded counterparts.

Keywords: bone defect, biological membrane, degradation, salt-leaching technique, tibia

Introduction

Repairing bone defects remains a major clinical problem in the fields of periodontology and oral implantology.[1,2] Guided bone regeneration (GBR) is a widely applied, effective approach to treat alveolar bone defects around dental implants.[3] Harnessing the endogenous regeneration potential of bone, the membrane used for GBR prevents the ingrowth of the epithelium or fibroblasts into the bone defect site[4–6] and acts as a space holder for delayed osteogenesis.[7] The components of GBR membranes should meet specific prerequisites in addition to biocompatibility, non-immunogenicity, and nontoxicity, such as cell occlusivity, tissue integration, space-maintaining ability, nutrient transfer, and ease of use in clinical settings.

Currently, two types of membranes are used in clinical applications: non-resorbable and resorbable membranes. Non-resorbable membranes, such as expanded polytetrafluoroethylene (e-PTFE), have proven to be very effective in preventing soft tissue invasion[8,9] but need to be removed in a second-stage operation. Resorbable membranes,

Correspondence: Wei Wu
Department of Oral & Maxillofacial Surgery, School of Stomatology, The Fourth Military Medical University, 145 West Changle Road, Xi'an 710032, Shaanxi, People's Republic of China
Fax +86 29 8477 6097
Email wuweidds@126.com

Yingliang Song
Department of Implant Dentistry, School of Stomatology, The Fourth Military Medical University, 145 West Changle Road, Xi'an, Shaanxi, 710032, China
Fax +86 029 8477 6454
Email sylfmmudds@163.com

submit your manuscript | www.dovepress.com
Dovepress
http://dx.doi.org/10.2147/IJN.S192167

such as collagen membranes, do not need to be removed and have a GBR effect.[10] In theory, the degradation time of resorbable membranes should be long enough to achieve bone regeneration before membrane disintegration. However, degradation rates are rapid and unpredictable, despite the use of various cross-linking techniques, and this impairs barrier function during the 4–6-month period required for complete healing and regeneration.[11] An important issue with collagen membranes and e-PTFE membranes is their weak mechanical properties; they frequently require reinforcement with titanium mesh or filling with less degradable hydroxyapatite in the targeted repair region. However, these materials require a second surgery for removal, and exposure/infection rates are as high as 20%–44%.[12,13] These limitations of current therapies have stimulated the development of new membrane materials. Synthetic membranes prepared using various materials, such as polyglycolides, polylactides, and copolymers, are sufficiently biocompatible and biodegradable for use as barrier membranes.[14–18] However, conventional fabrication techniques utilize toxic solvents that adversely affect cells and tissues if they are not completely removed. Furthermore, it is difficult to adjust the thickness, pore size, or external shape of fabricated scaffolds and to maintain architectural consistency.[19–21]

As a kind of heat-resistant cross-linking polyester, polyglycerol sebacate (PGS) is characterized by biocompatibility, elasticity to resist tissue compression, and flexible fabrication styles, including salt leaching and electrospinning. We therefore proposed that PGS could be an ideal biomaterial for GBR applications. We fabricated GBR membranes using PGS and investigated the impact of scaffold pore size on osteogenesis. PGS microporous membranes with various pore sizes were fabricated using the salt-leaching technique. Some related experiments in vivo have shown that microporous membranes with a pore size of 25–32 μm can not only promote osteogenesis but also increase volume, height, and compression modulus of bone.[21]

Materials and methods

Fabrication of PGS biological membranes with different pore sizes

PGS was dissolved in tetrahydrofuran (20%), and salt fusion and particulate leaching methods were used to fabricate porous scaffolds (thickness=1.0 mm, pore size=25, or 53 μm, porosity=90%), as described previously; the compressive modulus of the scaffolds was 4.05–1.30 kPa, as previously reported.[22] Scaffolds were cut into 2.25 cm^2 sheets (square) and autoclaved. Scaffolds were purified by serially soaking in 75%, 50%, and 30% ethanol, followed by soaking in PBS. A PGS biological membrane mold and holder were made using a standard microscope slide (1 mm thickness) by splicing and bonding. The holder was used when the PGS material was added dropwise. The hollow part of the mold was a square area of 15×15 mm.

Characterization of the PGS biological membranes by scanning electron microscopy (SEM) and tensile tests

The cross-section and longitudinal section of the PGS biological membrane were glued to an aluminum base with carbon fiber tape. After metal spraying, SEM was used for observations and imaging, and the pores of the PGS biological membranes were measured (n=5).

For the tensile test, the dehydrated PGS biological membrane was cut into a square block of 10×15 mm and fixed to the mechanical sensor on the frame of a small tensile tester using a self-regulating measurement clip. The free ends of the upper and lower clips were parallel. After the instrument was started, the speed of adjustment was 2 mm/min and the maximum tension was 10 N. The instrument continued to apply a tensile force of 2 mm/min until the biological membrane was broken. During the pull process, the instrument recorded the instantaneous pull and pull length values 250 times/second. The corresponding stress–strain curves were obtained by calculating the stress–strain values, and the elastic modulus of each biological membrane was calculated.

Animal groups and surgery

In this study, all animal experiments followed the strict procedures approved by the Institutional Animal Care and Use Committee of Fourth Military Medical University. The experimental procedure was approved by the ethics committee of the Fourth Military Medical University and was performed in accordance with the Code of Ethics (Ethical Accreditation No 2015 kq-022). All of the surgical operations were performed under systemic and local anesthesia, and all efforts were made to minimize suffering. Feeding and housing conditions were in accordance with standard animal care procedures. A total of 28 male New Zealand rabbits weighing 1,500–1,800 g were randomly divided into four groups: 25 μm PGS membrane (n=8), 53 μm PGS membrane (n=8), collagen (Bio-Gide, Geistlich, Switzerland) membrane (n=8), and a blank control group (n=4). Each rabbit underwent an operation on the left and right tibiae of the lower limb. Fourteen animals were sacrificed at each time point (4 and 12 weeks) for further analysis.

Based on the preoperative weight, 0.2–0.3 mL of sierra oxazine hydrochloride was injected into the local muscle. After the anesthesia took effect, 1.5–2 mL of preoperatively prepared 3% pentobarbital sodium was injected into the local muscle again. The rabbit was then completely anesthetized, and the skin at the proximal end of the tibia near the knee joint was prepared. The operative region was disinfected with 75% anhydrous ethanol. Securing the limbs, an incision was made on the sagittal plane of the proximal end of the tibia, followed by muscular dissection and complete exposure of the bone surface.

A bone defect with a diameter of 8 mm was created on the upper end of the tibia using a trephine bar (Microtech Inc., Tokyo, Japan) and covered with the prepared square membrane (12 mm in side length, n=4). The 25 μm PGS biological membrane, 53 μm PGS biological membrane, or collagen (Bio-Gide) membrane were placed on the surface of the surgical bone defect (Figure 1H). All biological membranes were cut in advance to obtain 12×12 mm blocks. In the blank control group, no material was used to cover the surgical bone defect. The periosteum and the muscle as well as the skin were sutured. During the operation, the operative area was washed and cooled continuously with 0.9% normal saline. Subsequently, the rabbit periosteum and epidermis were sutured with 6–0 and 4–0 silks, respectively. Thereafter, the rabbits were given free access to water and food under standard living conditions.

Micro-computed tomography (CT) scanning

After 4 and 12 weeks of in vivo incubation, four animals in each membrane group and two animals in the blank control group were sacrificed. Bone samples were harvested from the tibia using saws. Micro-CT scanning was performed to evaluate all bone samples. A three-dimensional visible representation of the constructs and animals was obtained and used for further analysis after reconstructing the imaging data using NRecon software (Version 1.5.1.4, Skyscan, Bruker Corporation, Karlsruhe, Germany). The ratio of the ossification volume to total construct volume (bone volume to tissue volume [BV/TV]) for each sample in different groups was compared using micro-CT software (Inveon Research Workplace, Siemens, Germany).

Histological observation

Bone samples were fixed with 4% paraformaldehyde for 24 hours. Fixed samples were decalcified in 10% EDTA for 15 days and dehydrated. After they were embedded in paraffin, the samples were cross-sectioned (6 μm thickness). Sections were dewaxed, hydrated in xylene and a series of alcohols, and stained with H&E and Masson's trichrome for general histology and bone evaluation. The stained sections were observed using a charge-coupled device (CCD) camera (DS-Fi2) equipped with an optical microscope (ECLIPSECI-L; Nikon Corporation, Tokyo, Japan). The image analysis system (Image-Pro Plus 6.0; Media Cybernetics Corporation, Maryland, USA) was used to quantitatively evaluate and analyze newly formed bone in bone defects. The percentage of new bone area was calculated by determining the new bone area as a proportion of the defect area.

Data analyses

All quantitative results are expressed as mean ± SD. Statistical analysis was performed using SPSS 17.0 (SPSS Inc., Chicago, IL, USA). Kruskal–Wallis ANOVA was used for comparisons among multiple groups, followed by Dunn–Bonferroni tests. The Mann–Whitney *U* test was used for two-group comparisons. Two-tailed *p*-values of <0.05 were considered statistically significant.

Results

Characteristics of the PGS porous membrane

The microarchitectures of the fabricated PGS membranes were evaluated by SEM (Figure 1A).

Highly porous structures could be observed on both sides and inner parts, and these pores were interconnected. Owing to the difference in pore size, the bulk densities of the 25 μm and 53 μm PGS membranes were 0.256±0.003 and 0.164±0.004 g/mm^3, respectively. The density of the commercial collagen membrane (Bio-Gide), used as a control, was 0.107±0.002 g/mm^3 (Figure 1E). Due to the elastomeric nature of heat-crosslinked PGS materials, an enhanced material density will inevitably increase resilience. The 25 μm pore size microstructure of the PGS membranes exhibited a much denser structure (Figure 1A) and thus a stronger ability to resist tissue compression. The conventional tensile test showed that the 25 μm PGS membrane and 53 μm PGS membrane had lower mechanical strength and breaking strain than the collagen membranes (Figure 1B and C), whereas no significant differences were observed between the 25 μm PGS membrane and 53 μm PGS membrane in this test. The elastic modulus of the 25 μm PGS membrane was 31.33±2.42 kPa and that of the 53 μm PGS membrane was 21.48±2.03 kPa, and these values differed significantly (n=5, $p<0.05$; Figure 1D).

An advantage of the porous structure is the adequate pathways for the passage of liquids and small molecules, which is

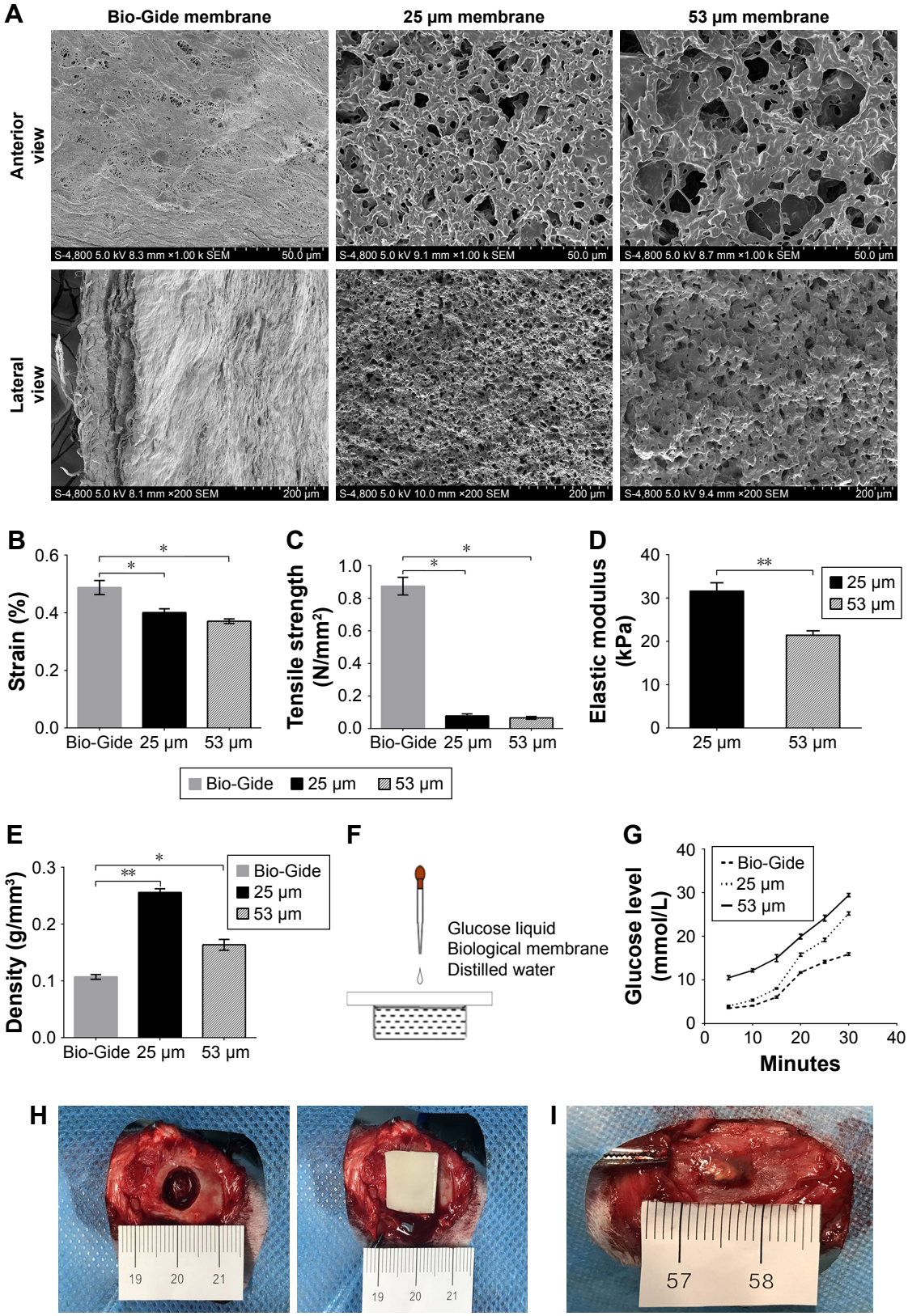

Figure 1 Structure and physical properties of the PGS membranes based on the GBR model of bone defects in rabbit tibia.

Notes: (**A**) SEM image of the cross-section of a freeze-dried 25 μm PGS membrane, 53 μm PGS membrane, and collagen membrane (Bio-Gide); scale bar, 50 μm or 200 μm. A suture pullout test (**B**) and tensile test (**C**) were performed (*$p<0.05$; mean ± SD; A: n=5, B: n=6, C: n=6). Compared with the control group, PGS membranes (25 μm and 53 μm) had lower mechanical strength and breaking strain. (**D**) Elastic modulus results are presented as mean ± SD (*$p<0.05$, mean ± SD, n=6). (**E**) Bulk densities are presented as mean ± SD (*$p<0.05$, **$p<0.01$, mean ± SD, n=6). (**F**, **G**) A permeability test was performed using PGS and Bio-Gide membranes. (**H**) Images of the surgical operation using the PGS membranes for the closure of tibial defects in rabbits. (**I**) Images of the bone sample for 25 μm PGS membranes at 4 weeks. There was a small piece of completely undegraded PGS membrane at the bone defect site.

Abbreviations: GBR, guided bone regeneration; PGS, polyglycerol sebacate; SEM, scanning electron microscopy.

favorable for tissue growth beneath the GBR membrane.[23–25] We thus compared the permeability of the membranes using an in vitro model (Figure 1F). As shown in Figure 1F, owing to the dense double-layer structure, Bio-Gide membranes showed a good blocking effect against macromolecules (the glucose molecules were approximately 0.7 nm). The PGS membrane with a 25 μm pore size exhibited better permeability than that of the Bio-Gide membrane; although glucose osmosis was not significantly different from that of the Bio-Gide membrane in the first 15 min, osmosis was significantly higher in the later stage. Owing to its loose and porous structure, the permeability of the 53 μm PGS membrane was the highest among the groups. These results confirmed that the porous PGS membrane is superior to the collagen membrane with respect to the rapid diffusion of glucose and other nutrients (Figure 1G).

Microporous PGS improved osteogenesis

To quantitatively evaluate the regenerated bone, micro-CT scanning images and analysis results at the end of 4 and 12 weeks after implantation are shown in Figures 2 and 3.

Rapid early bone formation was observed at 4 weeks postimplantation. The results showed that a thin layer of trabecular bone formed under both PGS membranes and collagen membranes and was evenly distributed in most of the defects (Figure 2A). The BV/TV of the samples at 4 weeks in the 25 μm PGS group was higher than that in the 53 μm PGS and collagen groups (Figure 2B) and was higher in the 53 μm PGS group than in the collagen group. Accordingly, trabecular thickness (Tb.Th) and trabecular separation (Tb.Sp) in the 25 μm PGS group indicated superior osteogenesis to that of the other two groups, and trabecular number (Tb.N) was the same as that of the

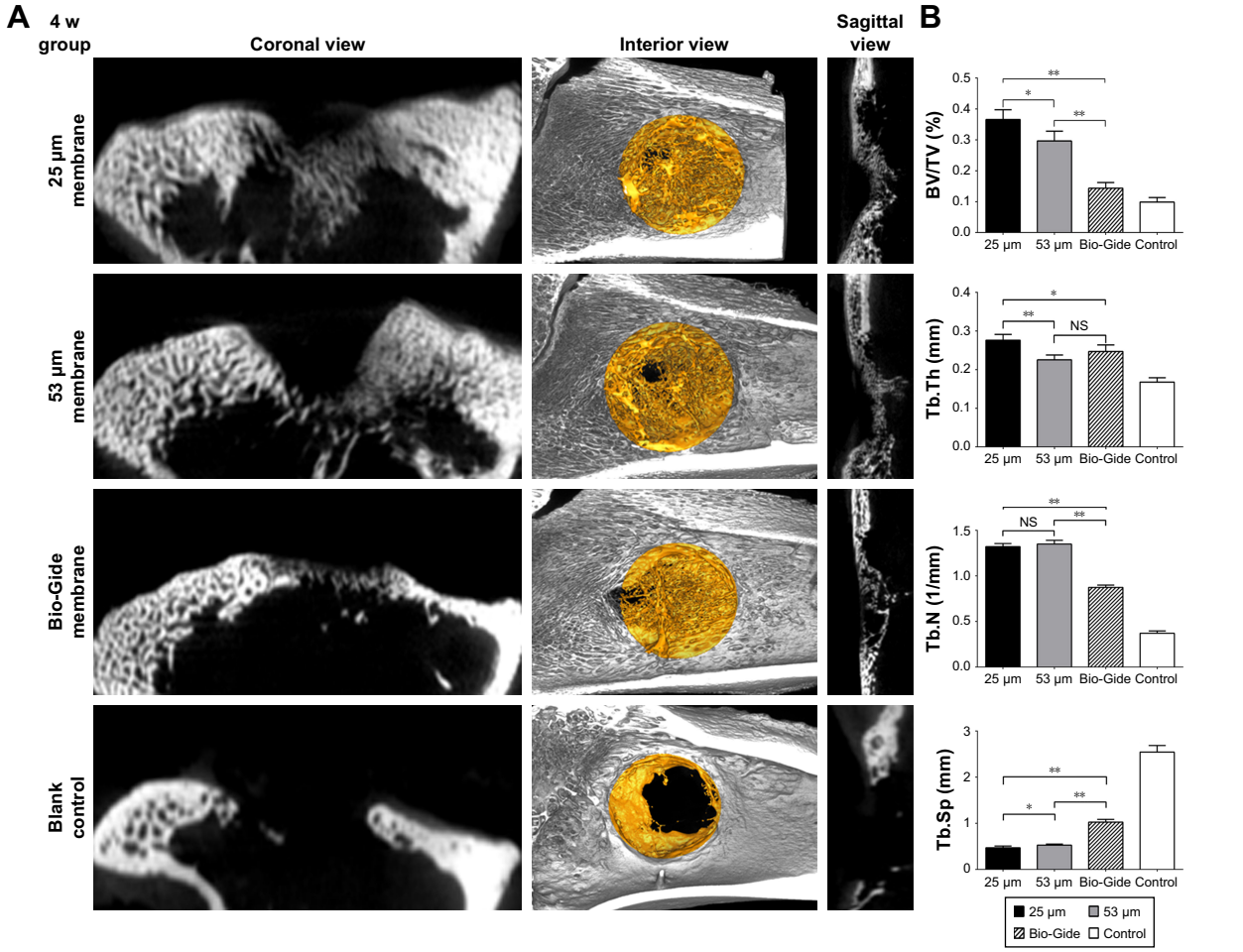

Figure 2 Micro-CT scanning images and analysis results at the end of 4 weeks.

Notes: (**A**) Bone defect models with or without membranes were scanned by micro-CT at 4 weeks postimplantation. In the 25 μm PGS, 53 μm PGS, and Bio-Gide membrane groups, regenerated cancellous bone covered the whole defect site after 4 weeks of implantation. (**B**) Volume ratios of regenerated bone were evaluated quantitatively in each group. BV/TV, Tb.Th, Tb.N, and Tb.Sp are presented as mean ± SD (*$p<0.05$, **$p<0.01$, n=16). At 4 weeks postimplantation, in the 25 μm PGS and 53 μm PGS groups, the volume ratios of newly formed bone were significantly higher than those in the Bio-Gide group and blank control group. "NS" indicates no significant difference among the PGS and Bio-Gide groups ($p>0.05$, mean ± SD, n=16).

Abbreviations: CT, computed tomography; PGS, polyglycerol sebacate; Tb.N, trabecular number; Tb.Sp, trabecular separation; Tb.Th, trabecular thickness; w, week; BV/TV, bone volume to tissue volume.

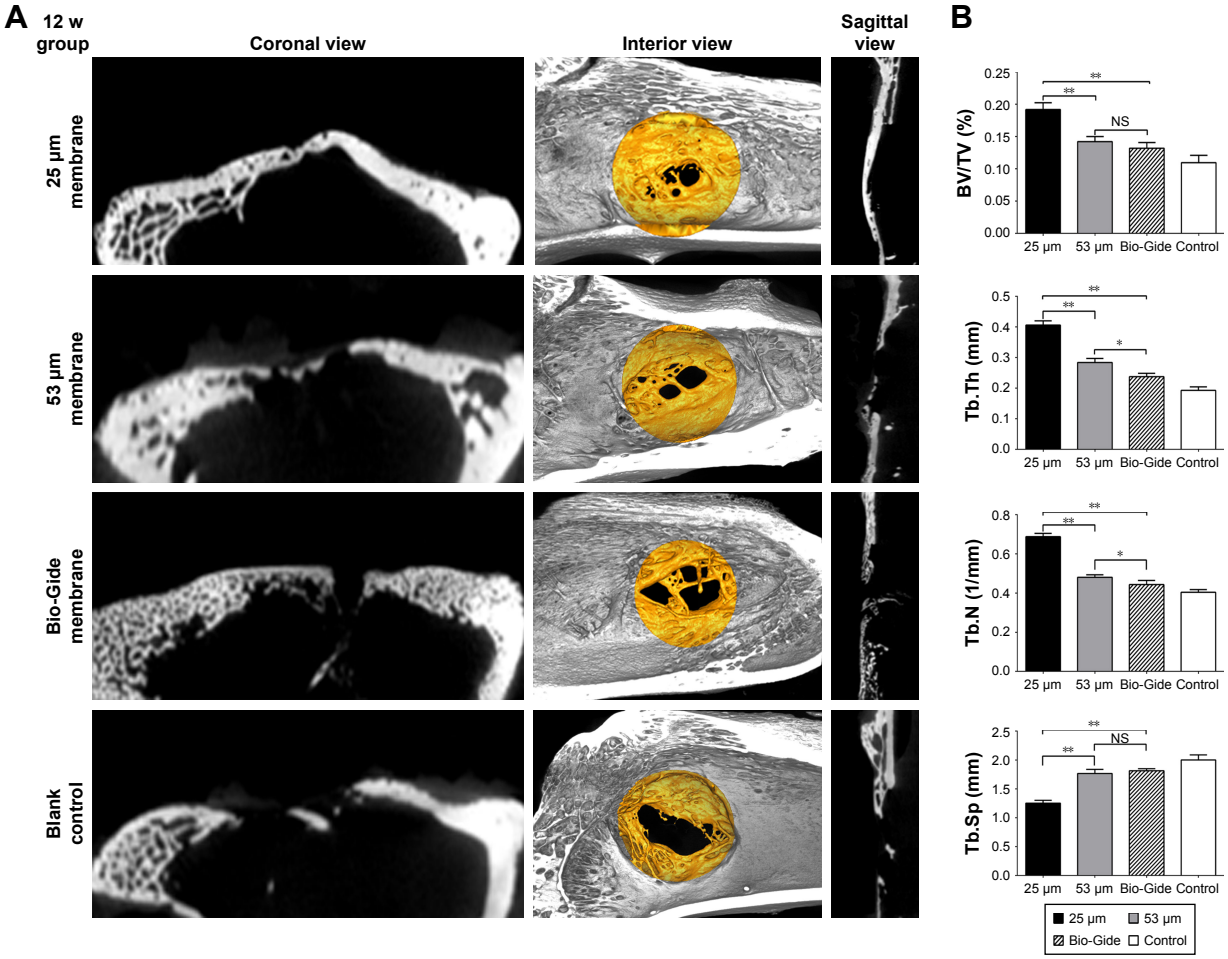

Figure 3 Micro-CT scanning images and analysis results at the end of 12 weeks.

Notes: (**A**) Bone defect models with or without membranes were scanned by micro-CT at 12 weeks postimplantation. In the 25 μm PGS, 53 μm PGS, and Bio-Gide membrane groups, regenerated mature lamellar bone covered the whole defect site after 12 weeks of implantation. (**B**) Volume ratios of regenerated bone were evaluated quantitatively in each group. BV/TV, Tb.Th, Tb.N, and Tb.Sp are presented as mean ± SD (*$p<0.05$, **$p<0.01$, n=16). At 12 weeks postimplantation, in the 25 μm PGS group, the volume ratio of newly formed bone was significantly higher than those in the 53 μm PGS group, Bio-Gide, and blank control groups. "NS" indicates no significant difference among the 53 μm PGS group and the Bio-Gide group ($p>0.05$, mean ± SD, n=16).

Abbreviations: CT, computed tomography; PGS, polyglycerol sebacate; Tb.N, trabecular number; Tb.Sp, trabecular separation; Tb.Th, trabecular thickness; w, week.

53 μm group. This result confirmed the osteoconductive property of the PGS membrane. At 12 weeks, the 25 μm PGS membrane guided the formation of lamellar bone. Micro-CT images clearly showed that the new bone grew from the lateral margins, and thickened trabecula formed within the defects in both PGS membrane groups (25 and 53 μm) and the collagen membrane group (Figure 3A). In the 25 μm PGS group, the new bone beneath the membrane almost completely covered the defect site. However, in the collagen membrane group or 53 μm PGS group, although the new bone beneath the membrane covered most of the defect areas, a portion was left uncovered. Quantitative analyses of trabecular thickness and trabecular separation showed that the distribution of regenerated bone under the PGS membranes was fairly uniform; the maximum trabecular thickness was 0.40±0.06 mm, and the minimum trabecular separation was 1.25±0.10 mm (Figure 3B). Furthermore, the trabecular thickness in the 25 μm membrane group was significantly greater than that in the other two groups, whereas the 53 μm PGS and collagen membrane groups exhibited similar values for Tb.Th and Tb.Sp.

Histological observation further verified these findings (Figure 4).

In the untreated control group, the healing areas of tibial defects were mainly bridged by fibrous connective tissue, and bone formation was limited to the edge of the host bone. Specifically, a three-layer bone structure was clearly visible in the PGS and collagen membrane groups. At 4 weeks, almost all of the bone defect areas in all treatment groups (25 μm PGS membrane, 53 μm PGS membrane, and collagen membrane) were almost entirely closed by immature trabecular bone. There were a greater number of small vascular channels in the new bone structure, which appeared to facilitate the differentiation of new bone

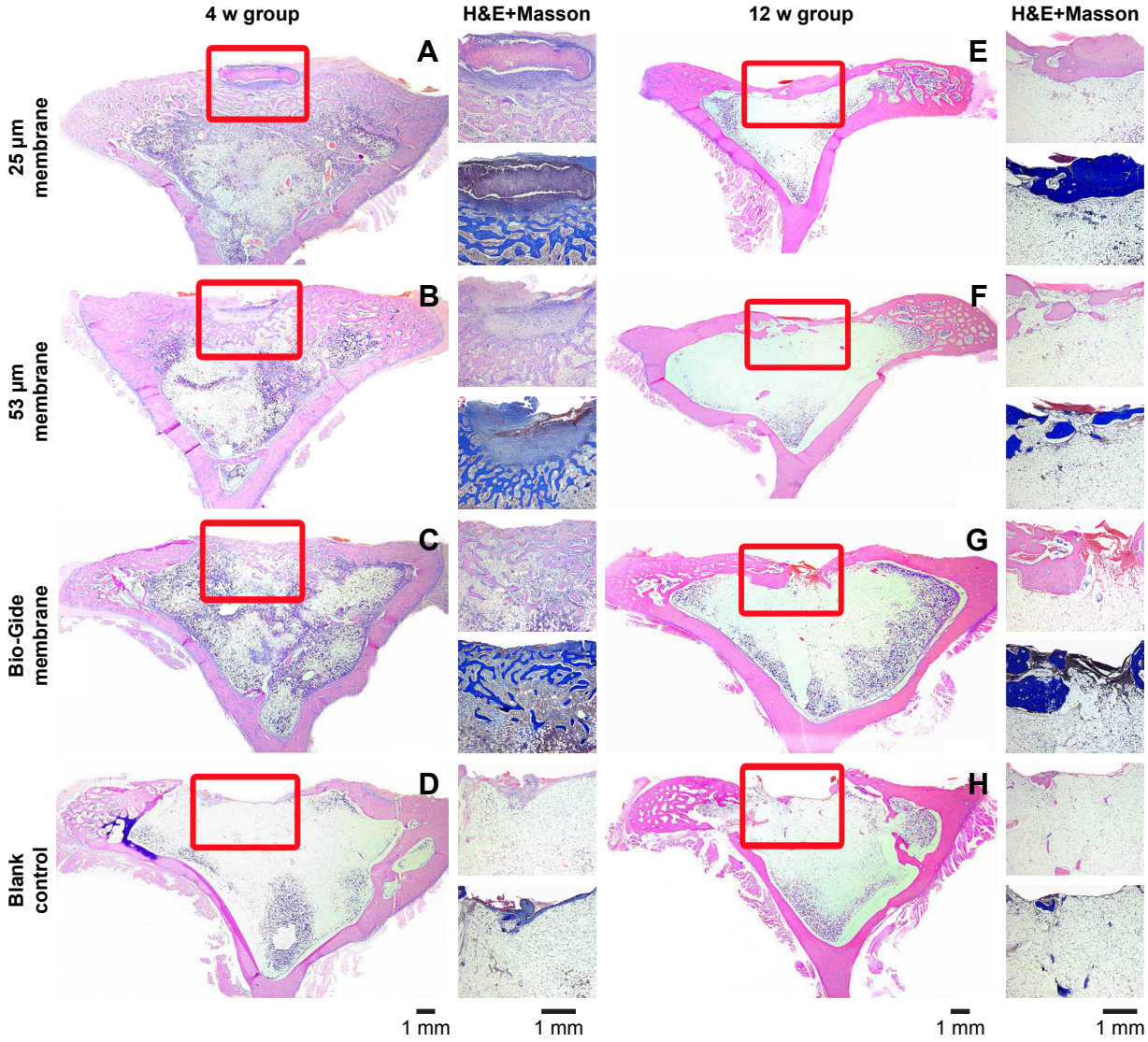

Figure 4 Histological analysis results at the end of 4 and 12 weeks. H&E-stained images of regenerated bone at 4 weeks (**A**–**D**) and 12 weeks (**E**–**H**) after membrane implantation. The entire images (left) and magnified images (right) were separated on both sides. The boxed areas in the images on the left show the lateral margin and central region of the rabbit tibia defect beneath the membranes. The images on the right show H&E staining and Masson's trichrome staining. In the tested membrane group, the transition of newly formed bone from cancellous bone to mature lamellar bone structure was observed.
Abbreviation: w, week.

from the host bone. However, the vertical height of newly formed trabecula varied significantly. Collagen membranes were completely absorbed, no inflammation was detected, and newly formed bone bridges without obvious collapse in the defect site were observed. Most of the 53 μm PGS membranes were degraded at 4 weeks, and fibrous tissues occupied the upper half of the newly formed trabecula, thus compromising the thickness of the new bone. Most of the 25 μm PGS membranes remained on the defect site, and a certain number of trabeculae formed beneath the PGS membrane, with no significant difference in the vertical height of bone as compared with that observed for collagen membranes. At 12 weeks, however, only the 25 μm PGS membrane guided the complete coverage of the defect by mature, lamellar bone, with adequate thickness as well as a smooth surface. The remainder of PGS membrane was completely degraded, and no inflammation was observed at cellular level. In the 53 μm PGS membrane and collagen membrane groups, subtotal repair with immature bone was observed, and the remaining unhealed area was covered by fibrous connective tissue.

Histological staining (eg, Alizarin red/von Kossa) is an important staining method to confirm the structural properties of bone matrix.[26] However, because the tissue sections in the experiment were decalcified sections, Alizarin red/von Kossa staining method was not used. In fact, in several studies, decalcified sections have been widely used in the identification of bone matrix structures.[20,27,28]

Discussion

Our goal was to develop an elastomeric GBR membrane that reduces hydroxyapatite or titanium mesh administration in clinical practice. We developed a biocompatible membrane using a tough and elastomeric polymer, PGS. The resultant biomaterials exhibited tunable pore sizes and high porosity, resulting in satisfactory resilience to external loading and favorable supportive performance when covering defects.

PGS not only has good osteogenic properties and biocompatibility[29,30] but also has good mechanical and selective osmotic properties as well as an easily defined material structure, which makes it a very promising material for GBR therapy. Therefore, in this study, we fabricated microporous PGS membranes with specific structures using a mold to investigate their effects on bone regeneration in GBR therapy.

During the GBR procedure, the PGS membranes effectively adhered to the bone tissue surrounding the defect, without additional grafting material and fixation pins. Based on a gross specimen inspection, the PGS membranes remained in place and maintained support and structural integrity before their complete degradation. Moreover, PGS membranes have better elasticity and mechanical compatibility with bone and surrounding tissues than those of hydroxyapatite filling-supported membranes and titanium-based membranes. This reduces the risk of exposure caused by mucosal perforation. It is worth mentioning that in our study, there was no significant swelling and inflammation in the healing area of bone defect in the PGS/collagen group as well as in the blank control group. This good prognosis reflects the good biocompatibility of PGS membrane to a certain extent.

As a kind of biodegradable polymer, the degradation period of PGS membranes ranges from 1 month to 2 months according to the pore size and interconnectivity. We found that the 25 μm PGS membrane was retained for a longer time than the 53 μm membrane. The difference in the microarchitecture of PGS membranes could explain the variation in degradation rates. Infiltrated macrophages are involved in PGS scaffold-mediated tissue remodeling.[31] A histological analysis confirmed that cell infiltration at as early as 4 weeks was significantly greater for the 25 μm membrane than for the 53 μm membrane, and this infiltration included macrophages, leukocytes, fibroblasts, and myofibroblasts. These results had been confirmed in our relevant studies.[32] We therefore concluded that infiltrating cells promoted resorption of the PGS membrane. Recently, a PGS membrane fabricated by electrospinning techniques showed significantly smaller pores than membranes fabricated by salt-leaching techniques, which have been reported to enhance mechanical strength. For the clinical application of GBR, early events, such as protein adsorption, cell adhesion, and apatite formation, in the process of new bone formation are vulnerable to the effects of microstructures, which are essential for subsequent osteoblast functions, such as cell proliferation and calcium mineral differentiation and deposition.[33] A study of biological activity and osteogenesis in vivo confirmed that the osteoconductivity of the PGS membrane is superior to that of biomembranes, which are prone to collapse. These results also suggest that PGS materials with a multilayered nanoarchitecture, if properly designed, can improve the osteogenic bioactivity and thus improve bone regeneration. Therefore, the rational design of pore size, including microarchitectures fabricated by the electrospinning technique, should be investigated in further studies.

An essential factor for GBR techniques is the maintenance of space at the defect site with the coverage of GBR membranes. Clot maintenance is critical for subsequent bone remodeling and osteogenesis. Interestingly, PGS membranes with different pore sizes and collagen membranes show significant differences in degradation rates. Moreover, the number and quality of trabecular bone have an important effect on the formation of new bone in the bone defect area. At 4 weeks, however, there was no significant difference in the number of new bone trabeculae between the PGS membrane group and the collagen membrane group. These results revealed the early therapeutic effect of biomaterial coverage on bone defects. At this time point, the collagen membrane was almost completely degraded; 70% of the 53 μm PGS membrane was degraded and 30% of the 25 μm PGS membrane was degraded on average (Figure 1I). Since the GBR membranes in individual groups degraded significantly after 4 weeks, there was obvious variation among groups at 3 months. Early collapse may decrease the vertical height of new bone. Additionally, early degradation may compromise bone quality owing to the mixture of fibroblasts. We thus concluded that the 25 μm PGS membrane is advantageous during the period from 4 to 12 weeks compared with earlier degrading counterparts.

The choice of animal models of bone defects is a very important consideration for studies of osteogenesis.[34] The regeneration of new bone in the defect area differs substantially between cranial flat bones and long bones owing to the different origin of embryonic tissue.[35] Cranial flat bone regenerates new bone by intramembranous ossification; however, both endochondral ossification and intramembranous ossification occur during long bone regeneration.[36,37] In the study by

Zaky et al,[30,33] they investigated polyglycerol sebacate (PGS) in vivo for the regeneration of a rabbit ulna critical size defect. Their study confirmed PGS to be osteoconductive contributing to bone regeneration by recruiting host progenitor/stem cell populations and as a load-transducing substrate. Also, they concluded that the material properties of PGS being closer to osteoid tissue rather than to mineralized bone. Based on the results of other studies, we boldly selected the GBR surgical area on the tibia of rabbits in our study and considered to further verify the bone regeneration ability of PGS materials in relatively large load areas. Due to dynamic mechanical loading, the formation of new bone in the bone defect area is faced with certain challenges. In the present study, at 4 weeks, there was a difference in early osteogenesis in defects shielded with different GBR membranes in vivo. Blood clot and callus quantities were significantly greater in the PGS microporous membrane group, while the collapse of the collagen membrane or macroporous PGS membrane obviously reduced osteogenesis. The difference further confirmed that the tibial defect model was appropriate to reveal the discrepancies in GBR physical properties.

These findings suggest a potential pathway for continued progress in PGS membrane-guided osteogenesis. Moreover, many studies have shown that synergistic signal transduction between the physical properties of biomaterials and growth factor signaling may accelerate bone healing.[38] Some scholars have proposed a strategy for the combination of biomaterials and low-dose bone morphogenetic protein (BMP) (<150 ng).[39] Of course, the safe use of growth factors is very important for clinical applications. Ongoing experiments include the incorporation of growth factors into the scaffold,[40] such as platelet-rich fibrin, a popular source of endogenous growth factors, for improved osteogenesis.

Conclusion

We believe that the degradation time and mechanical strength of PGS membrane can be well controlled by controlling the pore size of the PGS membrane, which provides the necessary time, space, and nutrients to assure the formation of new bone. Compared with the early degraded biomembrane, the 25 μm PGS membrane had obvious advantages in the protection of blood clots and the formation of new bone in 4–12 weeks.

Data availability statement

The datasets generated and analyzed during the current study are available from the corresponding author on reasonable request.

Acknowledgment

This research was supported by the National Natural Science Foundation of China (Grant No. 31370997/81470775) and the National High-tech R&D Program of China (863 Program, Grant No. 22001155AA020920).

Disclosure

The authors report no conflicts of interest in this work.

References

1. Draenert FG, Gebhart F, Mitov G, Neff A. Biomaterial shell bending with 3D-printed templates in vertical and alveolar ridge augmentation: a technical note. *Oral Surg Oral Med Oral Pathol Oral Radiol*. 2017; 123:651–660. doi:10.1016/j.oooo.2016.12.011
2. Jonker BP, Roeloffs MW, Wolvius EB, Pijpe J. The clinical value of membranes in bone augmentation procedures in oral implantology: A systematic review of randomised controlled trials. *Eur J Oral Implantol*. 2016;9:335–365.
3. Khojasteh A, Kheiri L, Motamedian SR, Khoshkam V. Guided bone regeneration for the reconstruction of alveolar bone defects. *Ann Maxillofac Surg*. 2017;7:263–277. doi:10.4103/ams.ams_76_17
4. Elgali I, Omar O, Dahlin C, Thomsen P. Guided bone regeneration: materials and biological mechanisms revisited. *Eur J Oral Sci*. 2017; 125:315–337. doi:10.1111/eos.12364
5. Benic GI, Bernasconi M, Jung RE, Hammerle CH. Clinical and radiographic intra-subject comparison of implants placed with or without guided bone regeneration: 15-year results. *J Clin Periodontol*. 2017; 44:315–325. doi:10.1111/jcpe.12665
6. Hoornaert A, d'Arros C, Heymann MF, Layrolle P. Biocompatibility, resorption and biofunctionality of a new synthetic biodegradable membrane for guided bone regeneration. *Biomed Mater*. 2016;11:045012. doi:10.1088/1748-6041/11/4/045012
7. Aloy-Prosper A, Penarrocha-Oltra D, Penarrocha-Diago M, Penarrocha-Diago M. Dental implants with versus without peri-implant bone defects treated with guided bone regeneration. *J Clin Exp Dent*. 2015;7: e361–e368. doi:10.4317/jced.52292
8. Chia-Lai PJ, Orlowska A, Al-Maawi S, et al. Sugar-based collagen membrane cross-linking increases barrier capacity of membranes. *Clin Oral Investig*. 2018;22:1851–1863. doi:10.1007/s00784-017-2281-1
9. Greenstein G, Carpentieri JR. Utilization of d-PTFE barriers for post-extraction bone regeneration in preparation for dental implants. *Compend Contin Educ Dent*. 2015;36:465–473.
10. Soldatos NK, Stylianou P, Koidou VP, Angelov N, Yukna R, Romanos GE. Limitations and options using resorbable versus nonresorbable membranes for successful guided bone regeneration. *Quintessence Int*. 2017;48:131–147. doi:10.3290/j.qi.a37133
11. Moses O, Vitrial D, Aboodi G, et al. Biodegradation of three different collagen membranes in the rat calvarium: a comparative study. *J Periodontol*. 2008;79:905–911. doi:10.1902/jop.2008.070361
12. Norowski PA Jr, Fujiwara T, Clem WC, et al. Novel naturally crosslinked electrospun nanofibrous chitosan mats for guided bone regeneration membranes: material characterization and cytocompatibility. *J Tissue Eng Regen Med*. 2015;9:577–583. doi:10.1002/term.1648
13. Chiapasco M, Zaniboni M. Clinical outcomes of GBR procedures to correct peri-implant dehiscences and fenestrations: a systematic review. *Clin Oral Implants Res*. 2009;20(Suppl 4):113–123. doi:10.1111/j.1600-0501.2009.01781.x
14. Kawakatsu N, Oda S, Kinoshita A, et al. Effect of rhBMP-2 with PLGA/gelatin sponge type (PGS) carrier on alveolar ridge augmentation in dogs. *J Oral Rehabil*. 2008;35:647–655. doi:10.1111/j.1365-2842.2008.01850.x

15. Liang SL, Cook WD, Thouas GA, Chen QZ. The mechanical characteristics and in vitro biocompatibility of poly(glycerol sebacate)-bioglass elastomeric composites. *Biomaterials*. 2010;31:8516–8529. doi:10.1016/j.biomaterials.2010.07.105
16. Stachewicz U, Qiao T, Rawlinson SCF, et al. 3D imaging of cell interactions with electrospun PLGA nanofiber membranes for bone regeneration. *Acta Biomater*. 2015;27:88–100. doi:10.1016/j.actbio.2015.09.003
17. Ribeiro C, Sencadas V, Areias AC, Gama FM, Lanceros-Mendez S. Surface roughness dependent osteoblast and fibroblast response on poly(L-lactide) films and electrospun membranes. *J Biomed Mater Res A*. 2015;103:2260–2268. doi:10.1002/jbm.a.35367
18. Zhang E, Zhu C, Yang J, et al. Electrospun PDLLA/PLGA composite membranes for potential application in guided tissue regeneration. *Mater Sci Eng C Mater Biol Appl*. 2016;58:278–285. doi:10.1016/j.msec.2015.08.032
19. Wu W, Allen RA, Wang Y. Fast-degrading elastomer enables rapid remodeling of a cell-free synthetic graft into a neoartery. *Nat Med*. 2012;18:1148–1153. doi:10.1038/nm.2821
20. Yoshimoto I, Sasaki JI, Tsuboi R, Yamaguchi S, Kitagawa H, Imazato S. Development of layered PLGA membranes for periodontal tissue regeneration. *Dent Mater*. 2018;34:538–550. doi:10.1016/j.dental.2017.12.011
21. Khosravi R, Best CA, Allen RA, et al. Long-term functional efficacy of a novel electrospun poly(glycerol sebacate)-based arterial graft in mice. *Ann Biomed Eng*. 2016;44:2402–2416. doi:10.1007/s10439-015-1545-7
22. Gao J, Crapo PM, Wang Y. Macroporous elastomeric scaffolds with extensive micropores for soft tissue engineering. *Tissue Eng*. 2006;12:917–925. doi:10.1089/ten.2006.12.917
23. Oh SH, Kim TH, Chun SY, Park EK, Lee JH. Enhanced guided bone regeneration by asymmetrically porous PCL/pluronic F127 membrane and ultrasound stimulation. *J Biomater Sci Polym Ed*. 2012;23:1673–1686. doi:10.1163/092050611X589518
24. Li J, Zuo Y, Man Y, et al. Fabrication and biocompatibility of an antimicrobial composite membrane with an asymmetric porous structure. *J Biomater Sci Polym Ed*. 2012;23:81–96. doi:10.1163/092050610X543159
25. Turkkan S, Pazarceviren AE, Keskin D, Machin NE, Duygulu O, Tezcaner A. Nanosized CaP-silk fibroin-PCL-PEG-PCL/PCL based bilayer membranes for guided bone regeneration. *Mater Sci Eng C Mater Biol Appl*. 2017;80:484–493. doi:10.1016/j.msec.2017.06.016
26. Hasegawa T. Bone cell biology assessed by microscopic approach. Bone mineralization by ultrastructural imaging. *Clin Calcium*. 2015;25:1453–1460.
27. Jeffries EM, Allen RA, Gao J, Pesce M, Wang Y. Highly elastic and suturable electrospun poly(glycerol sebacate) fibrous scaffolds. *Acta Biomater*. 2015;18:30–39. doi:10.1016/j.actbio.2015.02.005
28. Lysiak-Drwal K, Dominiak M, Solski L, et al. Early histological evaluation of bone defect healing with and without guided bone regeneration techniques: experimental animal studies. *Postepy Hig Med Dosw*. 2008;62:282–288.
29. Lin D, Yang K, Tang W, Liu Y, Yuan Y, Liu C. A poly(glycerol sebacate)-coated mesoporous bioactive glass scaffold with adjustable mechanical strength, degradation rate, controlled-release and cell behavior for bone tissue engineering. *Colloids Surf B Biointerfaces*. 2015;131:1–11. doi:10.1016/j.colsurfb.2015.04.031
30. Zaky SH, Lee KW, Gao J, et al. Poly(glycerol sebacate) elastomer supports bone regeneration by its mechanical properties being closer to osteoid tissue rather than to mature bone. *Acta Biomater*. 2017;54:95–106. doi:10.1016/j.actbio.2017.01.053
31. Wu W, Allen R, Gao J, Wang Y. Artificial niche combining elastomeric substrate and platelets guides vascular differentiation of bone marrow mononuclear cells. *Tissue Eng Part A*. 2011;17:1979–1992. doi:10.1089/ten.TEA.2010.0550
32. Yang X, Wei J, Lei D, Liu Y, Wu W. Appropriate density of PCL nano-fiber sheath promoted muscular remodeling of PGS/PCL grafts in arterial circulation. *Biomaterials*. 2016;88:34–47. doi:10.1016/j.biomaterials.2016.02.026
33. Zaky SH, Hangadora CK, Tudares MA, et al. Poly(glycerol sebacate) elastomer supports osteogenic phenotype for bone engineering applications. *Biomed Mater*. 2014;9:025003. doi:10.1088/1748-6041/9/2/025003
34. Li Y, Chen SK, Li L, Qin L, Wang XL, Lai YX. Bone defect animal models for testing efficacy of bone substitute biomaterials. *J Orthop Translat*. 2015;3:95–104.
35. Jiang X, Iseki S, Maxson RE, Sucov HM, Morriss-Kay GM. Tissue origins and interactions in the mammalian skull vault. *Dev Biol*. 2002;241:106–116. doi:10.1006/dbio.2001.0487
36. Shapiro F. Bone development and its relation to fracture repair. The role of mesenchymal osteoblasts and surface osteoblasts. *Eur Cell Mater*. 2008;15:53–76.
37. Kim S, Hwang Y, Kashif M, Jeong D, Kim G. Evaluation of bone regeneration on polyhydroxyethyl-polymethyl methacrylate membrane in a rabbit calvarial defect model. *In Vivo*. 2016;30:587–591.
38. Cipitria A, Salmeron-Sanchez M. Mechanotransduction and growth factor signalling to engineer cellular microenvironments. *Adv Healthc Mater*. 2017;6. doi:10.1002/adhm.201700052
39. Martino MM, Tortelli F, Mochizuki M, et al. Engineering the growth factor microenvironment with fibronectin domains to promote wound and bone tissue healing. *Sci Transl Med*. 2011;3:100ra89. doi:10.1126/scitranslmed.3002614
40. Keeney M, Chung MT, Zielins ER, et al. Scaffold-mediated BMP-2 minicircle DNA delivery accelerated bone repair in a mouse critical-size calvarial defect model. *J Biomed Mater Res A*. 2016;104:2099. doi:10.1002/jbm.a.35735